Reversible Graphene Metal Contact through Hydrogenation

Srivats Rajasekaran[1,2], Sarp Kaya[2,3], Frank Abild-Pedersen[4], Toyli Anniyev[2], Fan Yang[5], Dario Stacchiola[5], Hirohito Ogasawara[3] and Anders Nilsson[2,3,4]

[1] Department of Material Science and Engineering, Stanford University, Stanford, CA 94305, USA

[2] SIMES, SLAC National Accelerator Laboratory, 2575 Sand Hill Road, Menlo Park, CA 94025, USA

[3] Stanford Synchrotron Radiation Lightsource, SLAC National Accelerator Laboratory, Menlo Park, CA 94025, USA

[4] SUNCAT Center for Interface Science and Catalysis, SLAC National Accelerator Laboratory, 2575 Sand Hill Road, Menlo Park, CA 94025, USA

[5] Chemistry Department, Brookhaven National Laboratory, Upton, NY 11973 USA

We use x-ray spectroscopy and density functional theory to investigate the hydrogenation induced electronic structure changes in graphene on Pt(111). The atom specific properties of the spectroscopy allows for a direct projection of the band structure on to the carbon atoms which was compared with calculated density of states. Instead of the generally expected band opening behavior, we observe states at the Fermi level in the carbon projected density of states. Hydrogenation is accompanied by pinning of the graphene to the substrate through the formation of local C-Pt bonds which causes the graphene layer to become metallic upon hydrogenation.

Published in Phys. Rev. B 86, 075417

Work supported in part by US Department of Energy contract DE-AC02-76SF00515.

I. Introduction

Recently several approaches have been explored to alter the conductance of graphene and substrate-graphene composites through modulation of the electronic structure of graphene[1–4]. It would be useful to control the band gap of graphene but also to induce strong hybridization with a foreign metal in order to form strong metal contacts with high local conductivity. The effect of pristine graphene-metal interaction on the electronic properties of graphene is well understood[5]. A reduction in the graphene-metal contact resistance has been reported to occur as a result of thermal treatment[6]. This however could be due to the desorption of the impurities on the sample arising from the wet preparation techniques.

The control of band gap could be achieved through size confinements by utilizing graphene ribbons[7]. Other hypothesis has been to functionalize graphene with hydrogen to form local C-H bonds in order to open a band gap[1,4]. There have been attempts to utilize hydrogenation as means to tailor the electronic structure of graphene grown on a metal substrate[1,4,8]. While band opening through hydrogenation of single layer was reported for graphene/Ir(111)[1] and Au intercalated Ni(111)[4] substrates, it has also been suggested that hydrogenation leads to the formation of mid-gap impurity states for quasi free standing graphene[8]. Increasing the defect density for graphene on metals has indicated that the hybridization with the metal increases[9].

The structural changes accompanying the hydrogenation of graphene on late transition metal substrates has been studied with core level spectroscopy[10]. Hydrogenation through C-H bond formation resulted in the buckling of the graphene overlayer to accommodate the hybridization change. This distortion from a planar structure induces some carbon atoms to get closer to the substrate atoms, leading to an increased carbon-substrate interaction, which has been observed through surface core level shifts in x-ray photoelectron spectroscopy (XPS)[10]. Hence, the question is if hydrogenation of graphene on metals would induce a band gap opening or result in an increased metallic character through hybridization with the underlying substrate.

In this article we address how hydrogenation alters the electronic structure of graphene interacting weakly with Pt(111) using scanning tunneling microscopy (STM) in combination with XPS, x-ray absorption and emission spectroscopy (XAS, XES) and electronic structure calculations with density functional theory (DFT). The main advantage of x-ray spectroscopy is that it provides an atom specific way to locally probe the electronic structure, allowing for isolation of the electronic contributions of the underlying substrate from the graphene overlayer[11,12]. We observe finite states at the Fermi level in the carbon *p*-projected density of states (DOS) after hydrogenation of the graphene overlayer. The induced hybridization change in the hydrogenated graphene overlayer results in strong interaction between Pt and C atoms. The experimental findings together with DFT calculations clearly show that this strong hybridization with the substrate, due to symmetry change in local carbon bonding structure, gives rise to the observed states at the Fermi level. This reversible Pt-C interaction (via hydrogenation-dehydrogenation) could lead to a better graphene-metal contact. This can be viewed as two counteracting effects: one that leads to a broadening of the π electron band since the formation of local C-H bonds shift the π-electron states towards higher binding energy (BE), and another effect where the formation of C-Pt bonds restricts the π-band to become pinned to the Fermi level.

II. Experimental and computational methods

Single layer graphene (SLG) samples were prepared by the process described elsewhere[13]. Graphene was hydrogenated using commercial Omicron EFM-H atomic hydrogen cracking source at room temperature. The process of hydrogenation with deuterium and SLG with saturated atomic deuterium coverage are referred to as hydrogenation and H-SLG, respectively. We also refer deuterated carbon atoms to C-H. Saturation was confirmed through XPS measurements by observing no further change in C 1*s* XPS spectra with prolonged deuterium dose. Deuterium was used instead of hydrogen for obtaining accurate adsorption coverage using temperature programmed desorption (TPD) since hydrogen background pressure might interfere with the hydrogen TPD signal. Quantification of hydrogenation was obtained by calibrating against 2/3 ML p(3×3)-D structure on Cu(111)[14,15]. Graphene on Pt(111) was treated

with atomic deuterium and placed at the exact same position where Cu(111) was placed in front of the mass spectrometer. The saturation coverage was found to be 0.42 ML.

The x-ray spectroscopy measurements were carried out at BL 13-2 elliptical undulator beamline at Stanford Synchrotron Radiation Lightsource (SSRL). The experimental details of XAS and XES measurements at the C K-edge are described elsewhere[13]. STM studies were conducted in an Omicron variable temperature STM system at room temperature. The first principles calculations have been performed based on DFT. The grid-based projector-augmented wave method (GPAW) code was employed[16] and we have used the semi-empirical BEEF-vdW functional[17]. We used a 4×6×1 Monkhorst-Pack sampling of the Brillouin zone. Inner cores were replaced by projector-augmented wave method (PAW) pseudopotentials[18] and a uniform real-spaced grid with a spacing of 0.18 Å was used for the representation of the electronic wave functions. The Pt(111) surface and the graphene layer were modeled using the supercell slab approach with a 4×2 graphene sheet on a 4 layer (3×2) Pt(111) unit cell. For the hydrogen covered SLG every second carbon in the sheet were terminated by hydrogen to explicitly break the sp^2 symmetry of all carbon atoms. The induced strain on the graphene sheet from its equilibrium structure due to the small mismatch between the Pt(111) model system and graphene is found to be much less than 1% in both x and y. The distance between slabs is 16 Å and all structures were relaxed such that the average forces were below 0.05 eV/Å. The electronic structure of the systems considered in this paper has been analyzed by calculating the orbital projected DOS that we get directly from the projections of the Kohn-Sham eigenstates onto the atomic orbitals of the individual atoms. The resulting DOS are then plotted as a function of the energy relative to the Fermi-level.

III. Results and interpretation

Although the focus of the present article is the change in the electronic interaction between graphene and metals due to hydrogenation, it is essential that we briefly discuss hydrogenation induced geometric structure changes. Most graphene domains exhibit the superstructure lattice with a periodicity of 1.95 nm, which has been characterized as the $(\sqrt{63}\times\sqrt{63})\boldsymbol{R}19$ structure in a previous study by Enachescu et al.[19]. Bright and dark regions of

the honeycombs (Fig. 1(a)) indicate out of plane rippling of SLG as well as varying registry of the carbon atoms with respect to Pt(111) surface atoms. The morphology of SLG after hydrogenation is shown in Fig. 1(b). Ring-like structures were observed on top of the periodic structure of graphene. Most rings delocalized around the bright honeycombs of graphene while some coalesce to form elongated bright structures. Nonetheless, a Fourier transform of the STM image (inset of Fig. 1(b)) shows that the superstructure remains intact, in agreement with a previous study on the hydrogenation of graphene on Ir(111)[1]. The C 1*s* XP spectra of SLG and H-SLG are shown in Fig. 1(c). C 1*s* spectra for SLG on Pt(111) exhibit a narrow line width consisting of a single component corresponding to sp^2 hybridized carbon atoms. The two most important features of hydrogenation are the formation of C-H bonds and an increased C-Pt hybridization. We observe a C-H component at ~284.8 eV[20], a lower BE shoulder (~283.7 eV) due to defects, and a component which corresponds to C-Pt hybridization (~284.3 eV). Features observed in Pt $4f_{7/2}$ peak (Fig. 1(e)) directly manifest this C-Pt hybridization. The mutual decay of the Pt surface state and appearance of a higher BE shoulder at 71.4 eV, corresponds to the increased graphene-Pt interaction. This interaction, likely due to the overlap between the valence states of Pt and carbon. The deconvolution of C 1*s* XP spectra of H-SLG reveals the sp^2 (22%), C-H (42%), defect (10%) and C-Pt hybridized (26%) components. The spectral weights are self-consistent with the observed maximum deuterium coverage by TPD measurements (0.42 ML) and disappearance of surface component in Pt $4f_{7/2}$ spectrum. It should be noted hydrogenating a thicker sample (nominal thickness ~2ML graphene) resulted in a spectra with no defective component (not shown). However other spectra (XES-XAS) reported in this article remained the same (when normalized per carbon atom). Hence we can safely assume that this defective component does not play an important role in our interpretations and conclusions.

The dipole selection rule in XAS and XES processes is utilized to map σ and π symmetry resolved chemical bonding environments[12]. Since the excitation and de-excitation process involves the state localized on the core-excited C atom, the electronic structure is directly projected out in terms of C 2*p* local DOS in the carbon layer. We thereby have a direct separation between metal and carbon contributions to the overall band structure. C K-edge XAS selectively probes the 2*p*-projected unoccupied DOS (u-DOS, conduction band) while XES measures the occupied DOS (o-DOS, valence band). The 2*p*-projected carbon DOS of graphene

obtained by XES and XAS is shown in Fig. 2. The C 1*s* XPS binding energy provides the Fermi level for the system[12] and we have, for simplicity, chosen the sp^2 component. Although each specific component would have a different Fermi level this approximation will only lead to minor distortions and will not affect the main results.

Let us briefly discuss the σ and π symmetry XAS spectral changes due to hydrogenation. The resonant feature at 3.5 eV in π symmetry and quenching of π^* intensity (at 1.5 eV) are associated with formation of C-H bonds[20]. A change in C-C bond lengths is also expected; the shift of the σ^* states to lower energies indicates a C-C bond stretching[21]. An increase in π^* resonance intensity in σ geometry, and vice versa are observed, which are attributed to carbon atoms being tilted from the plane of pure graphene[20]. This distortion will result in an increased interaction between the graphene and the substrate. The increase of the absorption feature in π symmetry at 284.4 eV with hydrogenation (referred to as pre-edge), has been argued by other works to arise as a consequence of size confinement and hydrogen adsorption on the edge sites[22]. However this hypothesis is not necessarily true for graphene on Pt(111) (due to the large domain sizes[23]) and it was clearly shown that the pre-edge feature is attributed to the orbital interactions between graphene and Pt(111)[13], provides further evidence for increased interaction between H-SLG and Pt(111). The observations are in perfect agreement with recent XPS and non-symmetry resolved XAS observations[10].

Here we present the unique non-resonant XES spectra (Fig. 2) that directly reflect the o-DOS. The high symmetry critical points of graphene[13] are also indicated. The o-DOS of σ and π symmetry states can selectively be probed using angle resolved measurements[13].

The σ states of pure graphene dispersing along **K-M** and **M-Γ** symmetry lines contribute to the o-DOS as a broad peak centered at 7 eV with a tail towards the Fermi level[13]. The π states are concentrated closer to the Fermi level with almost no emission below 10 eV[13]. There are three important findings upon hydrogenation that can be observed in the o-DOS projected on the carbon layer. First we still observe a large DOS at the Fermi level in the π-states although it has been proposed that there should be a band gap opening[1,24]. Secondly we observe a reduction and energy shift of the π maximum density point to lower energies. This is accompanied by a

broadening of the π states reflected by the presence of higher emission in the region 8 eV to 12 eV below Fermi level. Thirdly, the hydrogenation leads to an increase in the σ o-DOS near Fermi level. This will have the same origin as in the above discussion regarding the XAS resonances with small symmetry mixing of σ and π states due to the distortion of the planar lattice upon hybridization change. Similar symmetry mixing in XES has been observed upon interaction of benzene on metal surfaces related to a re-hybridization, leading to a buckling of the ring structure[11].

The most significant finding is that, contrary to theoretical calculations that predict a band gap around **Γ** point for H-SLG[1,24], we find that a significant amount of states are formed at the Fermi level. A recent study utilizing resonant excited XES, or often denoted resonant inelastic x-ray scattering (RIXS) of graphene on Pt(111), has demonstrated that specific regions of the two-dimensional band structure can be selectively probed[13]. Here we make similar use of resonant excitations to look, in more detail, at the states close to the Fermi level. With excitation energy of 287.5 eV, states corresponding to C-H resonance are enhanced[13]. Fig. 3 shows that indeed, π o-DOS around the Fermi level is maintained and even enhanced after hydrogenation. Fig. 3 also shows the details of the π u-DOS above the Fermi level and we observe that it also increases after hydrogenation.

DFT results obtained using a semi-empirical functional that explicitly include non-local van der Waals interactions provide further insights into the experimental findings. Geometry optimized structure calculations (Fig. 4), performed at 0.5 ML hydrogen coverage for SLG on Pt(111), indicate that hydrogenation causes buckling of the graphene overlayer. Fig. 4 clearly shows that the Pt atoms on the surface of Pt(111) are pulled out towards the graphene layer and that the carbon atoms next to the hydrogenated carbon atoms gets closer to the surface Pt atoms (the closest distance between the atoms is 2.1 Å). This enhanced interaction between carbon and Pt atoms, is in agreement with our experimental findings, and has an important effect on the calculated DOS. Here we would like to point out that the maximum possible hydrogen coverage in experiments were ~0.4 ML. Also in the calculations, we are not exactly forming a diamond structure (for diamond structure we would need all C-C bonds to be 1.52 Å, the C-Pt bonds in H-SLG structure are 2.1 Å for C atoms on top of Pt and 2.35 Å for C atoms in “hollow” site of Pt).

We use 0.5 ML hydrogen coverage in the calculations just to drive home the importance of the H-SLG-Pt interaction in the observed DOS.

Fig. 5 displays the calculated carbon-projected symmetry-resolved σ and π DOS plots for H-SLG on Pt(111) (DOS of SLG on Pt(111) is also shown). The DOS plots agree well with the experimentally measured XES-XAS spectra. As expected, the σ and π DOS of SLG on Pt are shifted above the Fermi level (~0.4 eV in π DOS) due to charge doping and weak interaction with the substrate[13,23]. After hydrogenation, individual contributions of the carbon atoms in C-H and C-Pt bonds on the total DOS are displayed in order to elucidate the importance of the C-Pt interaction. The π DOS displays a downshift of the π states that is in accordance with other theoretical works[1,24]. However, only the states for C-H atoms display band opening. The states associated with C-Pt interactions show bonding and anti-bonding character in accordance with the d-band model[25,26]. Furthermore, we observe finite states at the Fermi level only for the carbon atoms in C-Pt bonds, which confirms that hybridization between SLG and Pt is the reason for states being observed at the Fermi level after hydrogenation. The change in the σ o-DOS for both C-H and C-Pt atoms is not that large but indicates an increased DOS closer to the Fermi level due to symmetry mixing with the π states in accordance with the XAS spectra. The increase in the u-DOS just above the Fermi level also validates our interpretation of the pre-edge in π XAS, which was attributed to charge transfer interaction rather than impurity adsorption.

The π dispersion at the **K** point of graphene grown on Ir(111) and Au intercalated Ni(111) have shown a band opening due to hydrogenation[1,4], but the change near the **K** point is not fully representative of the total changes in DOS. Although band opening was attributed to the confinement of pure graphene in ordered pattern of hydrogenated graphene[1], the important C-metal bond interaction found here was not considered. This could have been overlooked in the theoretical simulations since a simplified model was used by substituting the C-metal bonds with C-H bonds[1]. Since we clearly observe that the local C-H bonding downshifts the π-states, it is natural that graphene hydrogenated on both sides will give rise to a large band gap opening. Therefore, disregarding the pinning of graphene to the metal substrate and the disruption of long range 2D periodicity might not be suitable for estimations of band gap, especially for graphene grown on transition metal substrates. For smaller coverages (< 0.05 ML), it has been shown that

hydrogenation causes localized impurity states, and hence strong localization of π states might also lead to states being observed in this theoretically predicted gap region[2,8]. In our case, hydrogenation cannot be considered as an impurity adsorption and hence the states at the Fermi level should be correlated to the Fermi level pinning of graphene to the substrate as observed through the XES-XAS measurements and DFT calculations. It should also be mentioned that the common notion that more hydrogen adsorption causes a larger band opening could be most problematic[1,24]. The amount of hydrogen adsorption is related to the stabilization of the structural distortion, usually by hybridization of the H-SLG with the substrate, as shown here.

IV. Conclusions

Combining all the experimental and theoretical results, we conclude that hydrogenation of SLG/Pt(111) leads to metallization of SLG. The immediate consequences of hydrogenation induced changes in the DOS are the broadening and shift of the π states to lower energies and appearance of states near the Fermi level. The states near the Fermi level is not surprising since a C-Pt bond is formed between H-SLG and Pt(111) and metal character is thereby mixed into the graphene layer. This partially filled state will be responsible for the ohmic contact between metal and graphene layers.

Depending on the transition metal substrate, varying amounts of hydrogenation could be attained due to different C-metal interaction strength as expected from the d-band model. Hence hydrogenation could be used for either modulating in-layer conductivity (as demonstrated for graphene on SiC substrate[2]) or interlayer ohmic contact.

V. Acknowledgements

Part of this work was supported by the Global Climate and Energy Project operated by Stanford University and carried out at the Stanford Synchrotron Radiation Laboratory, a national user facility operated by Stanford University on behalf of the U.S. Department of Energy (DOE), Office of Basic Energy Sciences (BES). F.A.-P. wishes to acknowledge support from the (U.S.)

DOE, Office of BES. The work at BNL was financed by the US DOE, Office of BES (DE-AC02-98CH10086).

References

[1] R. Balog, B. Jorgensen, L. Nilsson, M. Andersen, E. Rienks, M. Bianchi, M. Fanetti, E. Laegsgaard, A. Baraldi, S. Lizzit, Z. Sljivancanin, F. Besenbacher, B. Hammer, T.G. Pedersen, P. Hofmann, and L. Hornekær, Nat. Mater. **9**, 315 (2010).

[2] A. Bostwick, J.L. McChesney, K.V. Emtsev, T. Seyller, K. Horn, S.D. Kevan, and E. Rotenberg, Phys. Rev. Lett. **103**, 056404 (2009).

[3] D.C. Elias, R.R. Nair, T.M.G. Mohiuddin, S.V. Morozov, P. Blake, M.P. Halsall, A.C. Ferrari, D.W. Boukhvalov, M.I. Katsnelson, A.K. Geim, and K.S. Novoselov, Science **323**, 610 (2009).

(4) Haberer, D.; Vyalikh, D. V.; Taioli, S.; Dora, B.; Farjam, M.; Fink, J.; Marchenko, D.; Pichler, T.; Ziegler, K.; Simonucci, S.; Dresselhaus, M. S.; Knupfer, M.; Büchner, B.; Grüneis, A. *Nano Lett.* **2010**, *10*, 3360–3366.

[5] P.A. Khomyakov, A.A. Starikov, G. Brocks, and P.J. Kelly, Phys. Rev. B **82**, 115437 (2010).

[6] T. Yu, C. Kim, C.-W. Liang, and B. Yu, IEEE Electron Device Letters **32**, 1050 (2011).

[7] V. Barone, O. Hod, and G.E. Scuseria, Nano Lett. **6**, 2748 (2006).

[8] D. Haberer, L. Petaccia, M. Farjam, S. Taioli, S.A. Jafari, A. Nefedov, W. Zhang, L. Calliari, G. Scarduelli, B. Dora, D.V. Vyalikh, T. Pichler, C. Wöll, D. Alfè, S. Simonucci, M.S. Dresselhaus, M. Knupfer, B. Büchner, and A. Grüneis, Phys. Rev. B **83**, 165433 (2011).

[9] M.M. Ugeda, D. Fernández-Torre, I. Brihuega, P. Pou, A.J. Martínez-Galera, R. Pérez, and J.M. Gómez-Rodríguez, Phys. Rev. Lett. **107**, 116803 (2011).

[10] M.L. Ng, R. Balog, L. Hornekær, A.B. Preobrajenski, N.A. Vinogradov, N. Mårtensson, and K. Schulte, J. Phys. Chem. C **114**, 18559 (2010).

[11] M. Weinelt, N. Wassdahl, T. Wiell, O. Karis, J. Hasselström, P. Bennich, A. Nilsson, J. Stöhr, and M. Samant, Phys. Rev. B **58**, 7351 (1998).

[12] A. Nilsson and L.G.M. Pettersson, Surface Science Reports **55**, 49 (2004).

[13] S. Rajasekaran, S. Kaya, T. Anniyev, H. Ogasawara, and A. Nilsson, Phys. Rev. B **85**, 045419 (2012).

[14] F. Greuter and E. Ward Plummer, Solid State Communications **48**, 37 (1983).

[15] E.M. Mccash, S.F. Parker, J. Pritchard, and M.A. Chesters, Surface Science **215**, 363 (1989).

[16] J. Enkovaara, C. Rostgaard, J.J. Mortensen, J. Chen, M. Dułak, L. Ferrighi, J. Gavnholt, C. Glinsvad, V. Haikola, H.A. Hansen, H.H. Kristoffersen, M. Kuisma, A.H. Larsen, L. Lehtovaara, M. Ljungberg, O. Lopez-Acevedo, P.G. Moses, J. Ojanen, T. Olsen, V. Petzold, N.A. Romero, J. Stausholm-Møller, M. Strange, G.A. Tritsaris, M. Vanin, M. Walter, B. Hammer, H. Häkkinen, G.K.H. Madsen, R.M. Nieminen, J.K. Nørskov, M. Puska, T.T. Rantala, J. Schiøtz, K.S. Thygesen, and K.W. Jacobsen, Journal of Physics: Condensed Matter **22**, 253202 (2010).

[17] J. Wellendorff, K.T. Lundgaard, A. Møgelhøj, V. Petzold, D.D. Landis, J.K. Nørskov, T. Bligaard, and K.W. Jacobsen, Phys. Rev. B **85**, 235149 (2012).

[18] G. Kresse and D. Joubert, Phys. Rev. B **59**, 1758 (1999).

[19] M. Enachescu, D. Schleef, D.F. Ogletree, and M. Salmeron, Phys. Rev. B **60**, 16913 (1999).

[20] A. Nikitin, L.-A. Näslund, Z. Zhang, and A. Nilsson, Surf. Sci. **602**, 2575 (2008).

[21] J. Stöhr, *NEXAFS Spectroscopy* (Springer, 1992).

[22] Z. Hou, X. Wang, T. Ikeda, S.-F. Huang, K. Terakura, M. Boero, M. Oshima, M. Kakimoto, and S. Miyata, J. Phys. Chem. C **115**, 5392 (2011).

[23] P. Sutter, J.T. Sadowski, and E. Sutter, Phys. Rev. B **80**, 245411 (2009).

[24] J.O. Sofo, A.S. Chaudhari, and G.D. Barber, Phys. Rev. B **75**, 153401 (2007).

[25] Hammer, B.; Norskøv, J. K. *Nature* **1995**, *376*, 238–240.

[26] A. Nilsson, L.G.M. Pettersson, B. Hammer, T. Bligaard, C.H. Christensen, and J.K. Nørskov, Catalysis Letters **100**, 111 (2005).

List of figures

Fig 1. STM images of (a) SLG and (b) H-SLG. Tunneling parameters: V=-0.60 V, I=0.1 nA. Inset of (b): Fourier transform of STM image of H-SLG. (c) C 1*s* XPS spectrum ($h\upsilon_{in}$ = 400 eV) of SLG (top) and 0.42 ML H-SLG (bottom) (d) Sketches of pinning of carbon atoms to Pt surface atoms after hydrogenation at the bright parts of the Moire (top – SLG on Pt(111), bottom – H-SLG on Pt(111)). (e) Pt $4f_{7/2}$ XPS spectra ($h\upsilon_{in}$ =165 eV) of SLG (top) and H-SLG (bottom). Spectra were deconvoluted using Gaussian-broadened Doniach-Šunjić functions. Assignments of C-Pt, C-sp^2,C-H, and defect components are made based on Pt $4f_{7/2}$ XPS, XAS (see below) and TPD measurements.

Fig 2. XES-XAS of SLG and H-SLG showing σ and π states, before and after hydrogenation. The C 1*s* binding energy position of the sp^2 hybridized state provides the Fermi level of the systems. Energy values are absolute relative to the Fermi level (dotted line). The normal emission XE spectra of SLG and H-SLG were normalized to the peak heights. The π component of the o-DOS was extracted by subtraction of the half normal emission spectra from grazing emission spectra after area normalization. Indicated with bars are the energy positions of certain high symmetry critical points for pure graphene. The critical points indicated are related to π (blue) and σ symmetry (green). XES was recorded with incident photon energy, $h\upsilon_{in}$=320 eV. Note that normalization between the XAS and the XES spectra are arbitrary.

Fig 3. Resonant π symmetry XES and XAS of SLG and H-SLG. The π symmetry XA spectra were normalized to the intensity maximum of the π^* resonance peak. Difference XE spectra form SLG and H-SLG were obtained by subtracting $2p_x$+$2p_y$ components (σ, normal emission) from $2p_x$+$2p_y$+$2p_z$ components (σ+π, grazing emission). Elastic emission peaks were cut for clarity. XES was recorded with $h\upsilon_{in}$=287.5 eV (excitation energy represented by blue arrow in the corresponding XAS).

Fig 4. DFT optimized structure for 0.5 ML H-SLG on Pt(111) showing (A) side view and (B) top view. Carbon atoms are colored green (carbon atoms bonded to hydrogen) and blue (carbon atoms bonded to Pt substrate). Hydrogen atoms are colored orange. Pt atoms are colored grey. C-Pt bonds (blue) are 2.1Å in length.

Fig 5. σ (top) and π (bottom) symmetry DOS calculated for geometry optimized structure SLG on Pt(111) and of 0.5 ML H-SLG on Pt(111). Individual contributions of carbon atoms bonded to hydrogen and Pt for H-SLG are also indicated. The total DOS for H-SLG is slightly offset to display the significance of contribution of carbon atoms bonded to Pt.

Figure 1

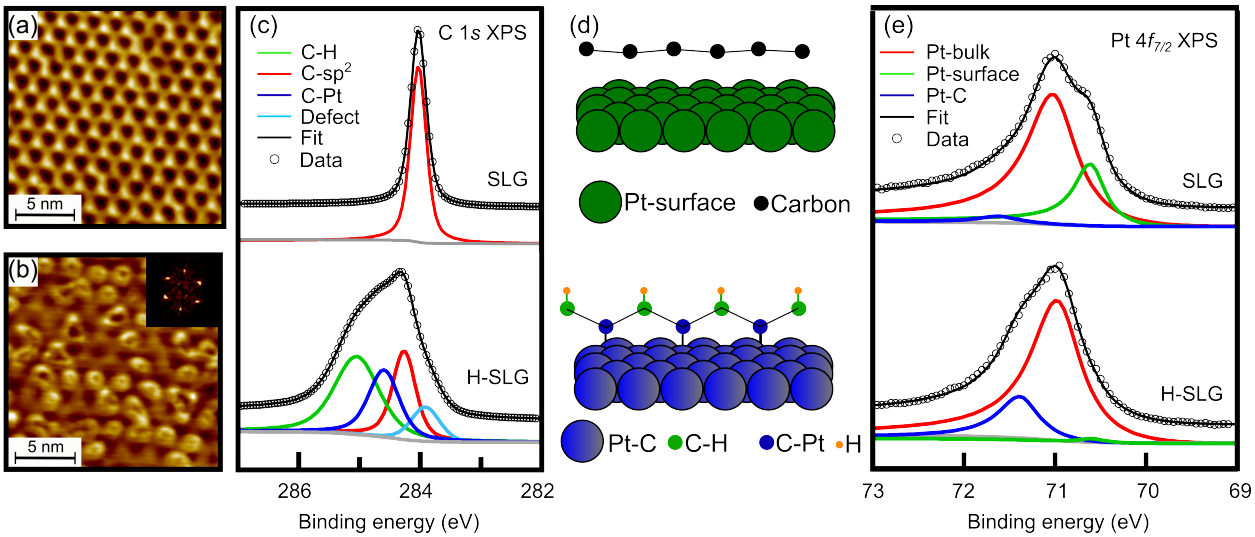
(a)
5 nm
(b)
5 nm
(c)
C 1s XPS
C-H
C-sp2
C-Pt
Defect
Fit
Data
SLG
H-SLG
286
284
282
Binding energy (eV)
(d)
Pt-surface
Carbon
Pt-C
C-H
C-Pt
H
(e)
Pt 4f7/2 XPS
Pt-bulk
Pt-surface
Pt-C
Fit
Data
SLG
H-SLG
73
72
71
70
69
Binding energy (eV)

1 Figure 2

2

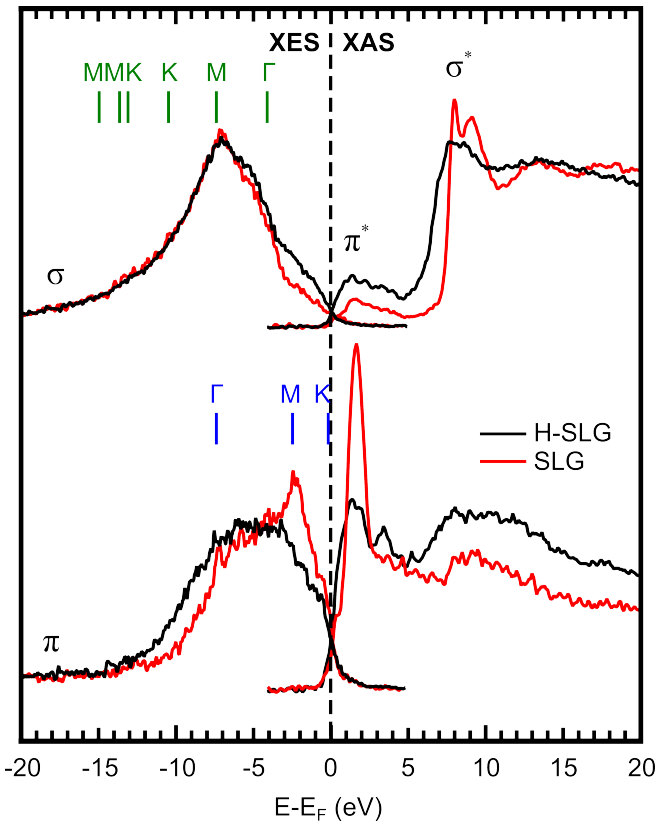

3

Figure 3

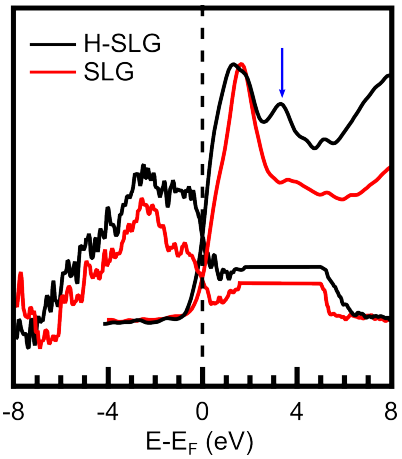

Figure 4

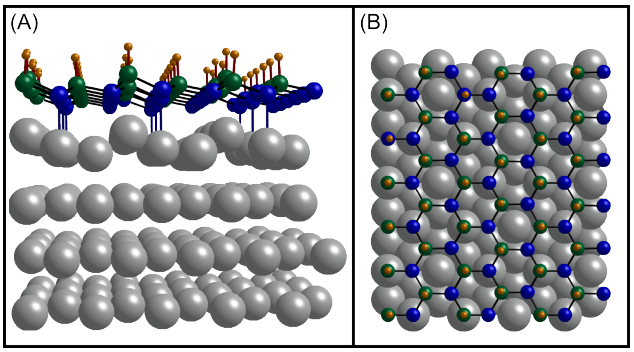

1 Figure 5

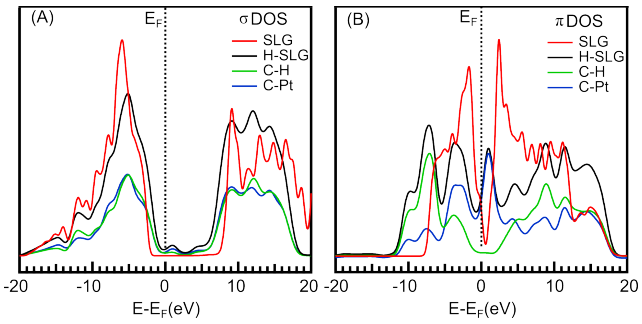
(A)
E_F
σDOS
SLG
H-SLG
C-H
C-Pt
-20
-10
0
10
20
E-E_F(eV)
(B)
E_F
πDOS
SLG
H-SLG
C-H
C-Pt
-20
-10
0
10
20
E-E_F(eV)

2